View metadata, citation and similar papers at core.ac.uk
brought to you by CORE
provided by NASA Technical Reports Server

NASA/TM-2005-213932
ARL-TR-3664

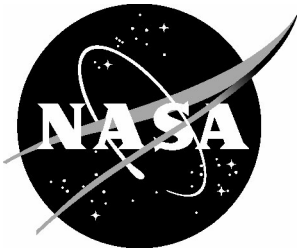

Identifying and Characterizing Discrepancies Between Test and Analysis Results of Compression-Loaded Panels

Robert P. Thornburgh
U.S. Army Research Laboratory
Vehicle Technology Directorate
Langley Research Center, Hampton, Virginia

Mark W. Hilburger
Langley Research Center, Hampton, Virginia

October 2005

The NASA STI Program Office . . . in Profile

Since its founding, NASA has been dedicated to the advancement of aeronautics and space science. The NASA Scientific and Technical Information (STI) Program Office plays a key part in helping NASA maintain this important role.

The NASA STI Program Office is operated by Langley Research Center, the lead center for NASA's scientific and technical information. The NASA STI Program Office provides access to the NASA STI Database, the largest collection of aeronautical and space science STI in the world. The Program Office is also NASA's institutional mechanism for disseminating the results of its research and development activities. These results are published by NASA in the NASA STI Report Series, which includes the following report types:

- TECHNICAL PUBLICATION. Reports of completed research or a major significant phase of research that present the results of NASA programs and include extensive data or theoretical analysis. Includes compilations of significant scientific and technical data and information deemed to be of continuing reference value. NASA counterpart of peer-reviewed formal professional papers, but having less stringent limitations on manuscript length and extent of graphic presentations.

- TECHNICAL MEMORANDUM. Scientific and technical findings that are preliminary or of specialized interest, e.g., quick release reports, working papers, and bibliographies that contain minimal annotation. Does not contain extensive analysis.

- CONTRACTOR REPORT. Scientific and technical findings by NASA-sponsored contractors and grantees.

- CONFERENCE PUBLICATION. Collected papers from scientific and technical conferences, symposia, seminars, or other meetings sponsored or co-sponsored by NASA.

- SPECIAL PUBLICATION. Scientific, technical, or historical information from NASA programs, projects, and missions, often concerned with subjects having substantial public interest.

- TECHNICAL TRANSLATION. English-language translations of foreign scientific and technical material pertinent to NASA's mission.

Specialized services that complement the STI Program Office's diverse offerings include creating custom thesauri, building customized databases, organizing and publishing research results ... even providing videos.

For more information about the NASA STI Program Office, see the following:

- Access the NASA STI Program Home Page at ***http://www.sti.nasa.gov***

- E-mail your question via the Internet to help@sti.nasa.gov

- Fax your question to the NASA STI Help Desk at (301) 621-0134

- Phone the NASA STI Help Desk at (301) 621-0390

- Write to:

  NASA STI Help Desk
  NASA Center for AeroSpace Information
  7121 Standard Drive
  Hanover, MD 21076-1320

NASA/TM-2005-213932
ARL-TR-3664

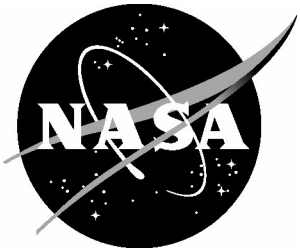

Identifying and Characterizing Discrepancies Between Test and Analysis Results of Compression-Loaded Panels

Robert P. Thornburgh
U.S. Army Research Laboratory
Vehicle Technology Directorate
Langley Research Center, Hampton, Virginia

Mark W. Hilburger
Langley Research Center, Hampton, Virginia

National Aeronautics and
Space Administration

Langley Research Center
Hampton, Virginia 23681-2199

October 2005

Available from:

NASA Center for AeroSpace Information (CASI)
7121 Standard Drive
Hanover, MD 21076-1320
(301) 621-0390

National Technical Information Service (NTIS)
5285 Port Royal Road
Springfield, VA 22161-2171
(703) 605-6000

Abstract

Results from a study to identify and characterize discrepancies between validation tests and high-fidelity analyses of compression-loaded panels are presented. First, potential sources of the discrepancies in both the experimental method and corresponding high-fidelity analysis models were identified. Then, a series of laboratory tests and numerical simulations were conducted to quantify the discrepancies and develop test and analysis methods to account for the discrepancies. The results indicate that the discrepancies between the validation tests and high-fidelity analyses can be attributed to imperfections in the test fixture and specimen geometry; test-fixture-induced changes in specimen geometry; and test-fixture-induced friction on the loaded edges of the test specimen. The results also show that accurate predictions of the panel response can be obtained when these specimen imperfections and edge conditions are accounted for in the analysis. The errors in the tests and analyses, and the methods used to characterize these errors are presented.

Introduction

To ensure high performance in the next generation of aerospace structures, it will be necessary to develop reliable, high-fidelity analysis tools to predict the buckling of thin-wall shells. For the past thirty years, buckling loads for shell structures have been obtained, to a large extent, by conducting linear bifurcation buckling analyses on idealized, geometrically perfect shell structures and by using empirical "knockdown" factors that account for the effects of geometric imperfections and other unknowns. Unfortunately, this analysis approach can result in overly conservative estimates of the buckling load of the shell and lead to a significant weight penalty in minimum gage design. Highly accurate or "high-fidelity" predictions of the structural response can be obtained when initial geometric imperfections, material property, thickness distribution, boundary conditions, load introduction effects, and other features are simulated with a high level of accuracy (ref. 1). These high-fidelity predictions typically require rigorous experimental validation before they can be used with confidence. However, validation-experiment requirements for compression-loaded composite curved panels are not yet fully mature. The primary reasons for the lack of maturity are that testing of curved panels requires complex fixtures to facilitate load introduction and edge support conditions can be difficult to characterize. These issues are significant because the characterization of load introduction and edge support conditions used for validation tests can affect the relevancy of a validation experiment.

Many theoretical and experimental studies of compression-loaded curved panels have identified discrepancies between test and analysis results (refs. 2-7). These discrepancies have been attributed to various effects such as improper simulation of boundary conditions, initial geometric imperfections, and geometry mismatch between the test specimen and the test fixture. For example, the effects of initial geometric imperfections on the buckling behavior of compression-loaded curved panels have been presented in the literature by a number of different authors (refs. 6-7) and it is widely accepted that these imperfections are a significant contribution to the discrepancies between predicted and experimentally measured buckling loads.

Khot and Bauld (ref. 6) found that experimentally measured buckling loads of curved composite panels were bounded by the corresponding predicted buckling loads for the case where the circumferential displacements on the curved loaded edges are unrestrained (free circumferential expansion) and for the case where these displacements are fully restrained. It was also noted in this study that some of the geometrically imperfect panels had to be forced slightly into the more geometrically precise test fixture, which produced an initial prestress and deformation states prior to loading. However,

the effects of this initial prestress and deformation was not characterized and was not accounted for in the analysis.

A recent numerical and experimental study by Hilburger et al. (ref. 7) identified cases where curved composite panels exhibited large magnitude out-of-plane prebuckling deformations and buckling loads that exceeded the classical linear bifurcation-buckling load. These response characteristics were contrary to previously known behavior associated with compression-loaded curved panels. In addition, the experimental buckling load was not bounded by predicted buckling loads for the case where the circumferential displacements on the loaded edges were unrestrained and the case where these displacements were fully restrained. In subsequent work (ref. 8), results from a numerical parametric study illustrating the effects of test-fixture-induced initial prestress and elastic edge restraints on the prebuckling and buckling responses of a compression-loaded, quasi-isotropic composite curved panel was presented. The elastic edge restraints were used to simulate the effects of test-fixture-induced friction on the loaded edges of the panel. The results showed that a wide variety of buckling and prebuckling behaviors could be obtained by varying the magnitude of the edge restraints and prestress. In particular, some of the results appeared to more accurately represent the experimentally measured results and illustrated the importance of properly characterizing the experimental test configuration. However, no experimental measurements were made to verify the actual as-tested boundary conditions of the panel.

The results presented in the literature reviewed herein indicated several sources for the observed discrepancies between test and analysis results. These discrepancies need to be well understood in order to develop experiments that are adequate for validating analysis methods for compression-loaded curved panels. The discrepancies have been attributed to initial geometric imperfection measurement errors, test-fixture-induced changes in specimen geometry, test-fixture-induced edge restraint due to friction, and nonuniform load introduction. To a large extent, these effects are not well understood. Thus, the objectives of the present paper are to describe the potential sources of discrepancies, how they affect high-fidelity modeling and validation experiments of compression-loaded panels, and the steps that were taken to quantify and minimize these discrepancies. Towards these objectives, a series of laboratory tests and finite-element analyses were conducted on flat and curved compression-loaded aluminum panels. Aluminum panels were chosen, as opposed to composite panels, for ease of manufacture and to verify that the observed discrepancies were not restricted to composite materials. Details of the experimental and analysis methods used in this study, and the initial observations that led to this study are described. Then, selected test and analysis results are presented that illustrate the effects of various sources of testing discrepancies on the panel response. Finally, new test procedures used to minimize the discrepancies are described.

Experimental Test Fixture

In this study, a set of four panels were fabricated from 0.125-inch-thick 6061-T6 bare aluminum. Two of the panels (AL-FLAT-1 and AL-FLAT-2) were flat and the other two (AL60-1 and AL60-2) were rolled to a radius of 60 in. The panel lengths were 14.75 in. and the circumferential arc-widths were 14.5 in. The loaded edges of the panels were machined flat and parallel to a tolerance of ±0.003 in. in order to provide uniform end loading during the tests. The test fixture for compression-loaded curved panels is shown in figure 1 along with a corresponding schematic of the fixture and displacement measurement instrumentation.

Initial geometric imperfections, thickness variations, and imperfections on the loaded edges of the panels were measured by using a coordinate measurement machine (CMM). While in the CMM the panels were held in a specially designed stand that gripped the panel at three or four points along the sides of the panel and held the panel stationary while it was being measured. The panels were measured outside the test fixture so that a larger portion of the panel's surface and the geometry of the loaded edges could be measured. In addition, this measurement stand could hold a panel in an undeformed, stress-free

configuration. Geometric data taken from a panel in this configuration allowed for subsequent characterization of panel and fixture geometry mismatch effects, specifically, test fixture-induced deformations and stresses in the panel.

The test fixture developed for this study was designed to replicate the idealized boundary conditions of a panel clamped along the loaded edges and simply supported along the sides (see figure 1). The curved loaded edges of the panel were clamped between a set of 3/8-in-thick clamping plates (g). These plates were precision machined to hold the curved edges at a precise radius-of-curvature and to also hold the panel aligned with the loading direction. The unloaded edges of the panel were supported by knife-edge supports (e) to simulate simply supported edges. The knife-edge supports were mounted in fixed support towers (d) that allowed the knife edges to rotate about the loading axis and maintain alignment during testing. The clamping plates on the loaded edges of the panel and the knife-edge supports were tightened against the panel to a finger tight condition. The loading plates (c, f) provided a surface for the clamping plates to be mounted to and a smooth surface for the panel to contact. The top loading plate (c) was free to move in the loading direction, relative to the rest of the fixture, by means of a set of linear bearings and guide posts (h).

Three direct-current differential transformers (DCDTs) were used to measure the displacement of the upper platen relative to the lower platen and one DCDT measured the out-of-plane center displacement of the panel. Two DCDTs were used to measure the lateral displacement near the top of the panel. In addition, a three-dimensional video image correlation system VIC-3D was used to measure the in-plane and out-of-plane panel deformations, and the strains. VIC-3D is a displacement and strain measurement technique developed by Correlated Solutions Inc. and uses a proprietary mathematical correlation method to analyze digital image data taken while a test specimen is subjected to load. Consecutive digital images taken during test are used to monitor changes in a high-contrast speckle pattern applied to the surface of the specimen as the specimen is loaded. The image data is processed to produce in-plane and out-of-plane full-field displacements and full-field in-plane surface strains.

Finite-element Model and Analysis Methods

The panels presented in this study were analyzed with the STAGS (STructural Analysis of General Shells) finite-element analysis code (ref. 9). STAGS is designed for the static and dynamic analysis of general shells and can include the effects of both geometric imperfections and nonuniform wall thickness in its analysis. The panel is defined by an x-y-z curvilinear coordinate system with the origin at the center of the panel, as illustrated in figure 2. The positive x-axis is directed along the axis of the panel towards the top of the panel; the z-axis is directed outward, normal to the surface of the panel and the y-axis is circumferential coordinate. Displacements u, v and w refer to the mid-surface axial, circumferential and out-of-plane displacements respectively. The panel length, width, and radius are defined as L, W, and R, respectively. Both flat and 60-in-radius curved panels were modeled, and the lengths and widths were 14.75 in. and 14.5 in., respectively. The panels were modeled assuming nominal material properties as follows: Young's modulus E = 10.0 Msi, and Poisson's ratio ν = 0.33. The measured initial geometric imperfections and thickness variations were included in the finite-element model by using user-defined shell wall and imperfection subroutines. Test fixture support conditions along the clamped edges and knife-edges were also defined by a user-defined load subroutine that provided a convenient means of applying nonuniform loading conditions that arise due to the imperfection. In addition, the subroutine was used to apply displacements on the panel edges to simulate the effect of putting a geometrically imperfect panel specimen into a more geometrically precise test fixture. The subroutine specifies displacements on the edges of the panel to be equal to the negative of the imperfection values from the appropriate rows or columns of nodes associated with the four boundaries. Thus, the deformed geometry of the panel (initial geometry plus imperfection) is forced to conform to the geometry of the fixture, which was assumed to be perfect (see figure 3). These boundary

conditions remain constant throughout the loading of the panel and the end-shortening displacement is introduced through a second load set. The knife-edge-support conditions were simulated by prescribing a displacement w along a line 3/16 in. from each unloaded edge of the panel and the clamped edge conditions were applied in the boundary regions that extend 3/8 in. in from each loaded edge as shown in figure 2. The compressive load is introduced by applying a uniform end shortening displacement Δ to one end of the panel while holding the other end of the panel fixed on the boundary; that is $u(-L/2, y) = \Delta$ and $u(L/2, y) = 0$.

Previously Observed Discrepancies Between Test and Analysis

A series of tests were planned, prior to this investigation, to study the effects of laminate orthotropy and cutout size on the response of compression-loaded, composite laminated, curved panels with circular cutouts. Finite-element analysis predictions of the response of the panels were obtained that included the effects of measured geometric imperfections and test-fixture induced panel deformations and pre-stress. Preliminary tests were conducted with composite curved panels without cutouts and significant discrepancies between test results and predictions were identified that warranted further study. A typical example of the observed discrepancies between the predicted and measured load-end-shortening response curves and load-center-displacement response curves for a compression-loaded composite laminated panel are shown in figures 4 and 5, respectively. This composite panel was 14.75 in. in length and 14.5 in. in width, with a $[0_2/\pm45]_{3s}$ stacking sequence and had a nominal thickness of 0.13 inch and a radius of 60 inches. The panel was constructed out of AS4/3502 graphite-epoxy tape. Nominal lamina properties include a longitudinal modulus $E_1 = 18.5$ Msi, transverse modulus $E_2 = 1.6$ Msi, in-plane shear modulus $G_{12} = 0.83$ Msi, and Possion's ratio $\nu_{12} = 0.35$. The predicted load-shortening response and load-center-displacement response of the panel indicated a linear prebuckling response and inward snap-through behavior that is typical for compression-loaded curved panels. In contrast, the experimentally measured results indicated nonlinearity in the prebuckling region of the load–end-shortening response curve, outward displacements from the onset of loading, and a buckling load that exceeded twice the predicted buckling load.

As noted in the introduction and in references 7 and 8, a number of phenomena can cause shallow curved panels to exhibit the behavior observed in the tests. Examples include initial geometric imperfection measurement errors, test-fixture-induced changes in specimen geometry, test-fixture-induced edge restraint due to friction, and nonuniform load introduction. Since both geometric imperfections and test-fixture-induced panel deformations and pre-stress had been included in the model, it seemed likely that the discrepancies were being caused by test-fixture-induced friction along the loaded edges in a similar manner to that described in References 7 and 8. However, other potential contributions to the observed discrepancies were also identified in these tests. In particular, there were cases where the measured panel shape of the panel mounted in the fixture obtained from the VIC-3D video image correlation system prior to testing did not always agree with the corresponding predicted panel shape obtained from a finite-element analysis. If the initial as-tested geometry of the panel was not being modeled accurately, then errors would be expected in the predicted panel response, which is highly sensitive to initial out-of-plane geometric imperfections. In addition, it was difficult to hold the panel shape constant while measuring the initial geometric imperfection with the CMM machine, because the force of the CMM probe caused slight bending of the panel during measurement. This error in the imperfection shape measurement could lead to inaccurate analysis results that were based on these measurements. Finally, studies on the buckling of thin-walled compression-loaded composite cylinders (see reference 1) suggest that the panels considered herein could also be sensitive to nonuniform load introduction that can occur when the loaded ends of the specimen are not flat and parallel. However, these end imperfections were not characterized for these composite panels and were not accounted for in the analysis predictions.

A subsequent set of tests and analyses were conducted to characterize and determine the effects of these errors on the response of compression-loaded flat and curved aluminum panels and the results of these tests are presented in the following sections. Specifically, results are presented that illustrate the effects of test-fixture and panel geometry mismatch effects such as test-fixture-induced changes in panel geometry and pre-stress, errors in imperfection measurements, effects of test-fixture-induced friction on the loaded boundaries, and effects of nonuniform load introduction on the panel response.

Results and Discussion

Effects of imperfection measurement errors

Initial geometric imperfections, thickness variations, and imperfections on the loaded edges of the panels are measured prior to each test by using a coordinate measurement machine (CMM). The panels are mounted in a specially designed measurement stand that grips the panel at three or four points along the sides of the panel (see figure 6). The panels are measured outside the test fixture so that a large portion of the panel's surface can be measured. In addition, this measurement stand can hold a panel in an undeformed stress-free configuration. Measurement data taken from a panel in this configuration allows for subsequent characterization of any panel and fixture geometry mismatch effects, specifically, test fixture-induced deformations and stresses in the panel.

In order to measure the geometric imperfection of a panel with the CMM, the panel must be held fixed while a measurement probe contacts its surface. Ideally, the panel would be restrained in the measurement stand at just three points, so that the gripping forces of the fixture would not induce any deformation of the panel. In addition, the magnitude of the contact force from the probe is small (typically less than 0.1 N) and the CMM software has features to minimize the measurement error due to surface deformation. However, thin panels are relatively flexible when being subjected to out-of-plane contact forces and measurements using this procedure produced noticeable errors because the panel deformed under the contact force. This measurement error was most evident when the geometry measurements from both sides of the panel were used to determine the thickness variation over the surface of the panel. Both surfaces deformed in the inward normal direction during the measurement and the thickness data, obtained by subtracting the inner mold line (IML) from the outer mold line (OML) of the panel, erroneously indicated a thinning of the panel away from the fixture support points. Although this measurement error was only a few thousandths of an inch for a 0.125 in. thick panel, it was enough to invalidate this thickness data for use in the finite-element analysis.

The solution to this problem was to restrain the panel at four points instead of three. By gripping the panel at two points on the left and right sides, the support condition was stiff enough to eliminate the error in the thickness measurement. The drawback to this method is that it is possible to deform the panel and create an artificial twist in the mid-surface imperfection measurement. This twist can be minimized by first gripping the panel securely at three of the points and then carefully restraining the panel at a fourth point. Some amount of deformation is still expected to occur as a result of the constraints, however, this was deemed to be acceptable, since a small twisting imperfection was not expected to change the predicted response of the panel significantly enough to invalidate the analysis.

In order to confirm this expectation, a simple comparison was made between a model of a typical panel and one that also included a large artificial twist in the mid-surface imperfection. The comparison was made for a flat aluminum panel and a 60-in-radius curved panel. The panels were first modeled by including the measured geometric imperfection and thickness variation. Then the model was modified to include the effects of a twist to the initial geometric imperfection of the form

$$\Delta_{imp} = \delta_{twist} \frac{\xi \eta}{2} \tag{1}$$

where ξ and η are normalized longitudinal and transverse surface coordinates, respectively, and vary between ± 1 over the surface of the panel. The magnitude of the twist, δ_{twist}, was chosen to be 0.1 in., which was an order of magnitude larger than the worst case error expected in the CMM data.

The predicted results for the aluminum panels with and without a twist imperfection are shown in figures 7 and 8. Figure 7(a) shows the load versus out-of-plane deformation response at the center of the flat panel and figure 7(b) shows the corresponding load versus end-shortening response. Figures 8(a) and 8(b) show the corresponding results for the 60-in-radius curved panel. The results indicate that the large twist imperfection causes only a slight change in the predicted response of the flat and curved panels considered herein. In particular, there is only a difference of about one percent in the buckling load of the curved panel and the end-shortening curves. Since the twist error used in this comparison is an order of magnitude larger than the worst-case error expected for the CMM data, the error caused by clamping a panel in order to measure it in the CMM should not significantly affect the accuracy of the predicted panel response.

Effects of test-fixture-induced changes in specimen geometry

Results from several panel tests indicated that the measured shape of the panel mounted in the fixture obtained from a VIC-3D video image correlation system prior to testing did not always agree with the corresponding predicted in-the-fixture panel shape obtained from a finite-element analysis. It was determined, through repeated independent CMM measurements, that the geometry of the specimens was known to a high degree of accuracy. This result suggested that there might be some geometric imperfections in the test fixture or that the interaction between the test fixture and the test specimen was not well understood, and thus could affect the validity of the assumed boundary conditions used in the analysis models. Therefore, a series of measurements were made in the CMM to determine the geometric accuracy of the test fixture and how the specimen deforms when it is placed into the test fixture prior to loading.

First, the geometric accuracy of the fixture was examined. In particular, measurements were taken to verify that the fixture had been manufactured to the correct tolerances for flatness and perpendicularity. The fixture support towers (see Fig. 1) were measured to be offset 0.00196 in. to the panel left, relative to the center of the fixture base plate (left and right directions are defined relative to a view of the panel OML). The knife-edge supports were offset 0.00318 in. to the panel left and the left knife-edge support is tilted 0.0382° towards the panel front, and the right knife-edge support was tilted 0.0199° towards the panel front. These misalignments are not critical to the function of the fixture, but could be significant when other measurements or alignments are referenced from them. The right knife-edge support was measured to be almost perfectly aligned with the loading direction, but the left support was found to be tilted 0.046° towards the panel front (or about 0.010 in. from top to bottom of the knife edge). This is likely a small enough deviation that results would not be affected, but it can be compensated for by small adjustments of knife-edge set-screws.

Next, it was discovered that the 3/8-in-thick clamping plates used to clamp the loaded edges of the panel had inaccurately machined bearing surfaces. Although they formed the correct radius of curvature, the bearing surface was not perfectly square. In particular, a deviation from perpendicular of as much as 0.003 in. across the 3/8-in-thick clamping plate was measured. This imperfection on the bearing surface corresponds to an angle of approximately 0.5 degrees. Thus, when the panel was clamped in the fixture, the top loading plate would tilt forward or back, depending on the imperfection shape on the clamping plate bearing surface and created a localized bending near the top of the panel when the panel was loaded. As a result of this discovery the clamping plates were all re-machined by a wire EDM

(electrical discharge machining) procedure, resulting in clamping surfaces that were perpendicular to within the accuracy of the CMM (a few ten thousandths of an inch).

Once the geometry of the fixture was verified, a numerical and experimental study was performed to determine the accuracy of the predicted in-the-fixture shape of the panel. A finite-element analysis was used to apply displacements on the panel edges in order to simulate installing a geometrically imperfect panel specimen into a more geometrically precise test fixture. A flat panel (AL-FLAT-2) and a 60-in-radius curved panel (AL60-1) were evaluated in this study. A prediction of the in-the-fixture shape of each panel was obtained as follows. First, the measured geometric imperfection of the unrestrained panel was incorporated into the finite-element model. Then, displacements were applied to the four edges of the panel to simulate the installation of the panel into the fixture. These displacements were applied to the panel by using a user-defined subroutine that defined the displacements to be equal to the negative of the measured geometric imperfection values from the appropriate rows or columns of nodes associated with the four boundaries. Following this procedure, the geometrically imperfect panel was forced to conform to the idealized perfect geometry of the fixture. In the experiment, the panels were installed into the fixture by securing one edge at a time and the panel geometry was measured with the CMM as each edge was secured. The edges were secured in the following order: bottom clamped edge, right knife edge, left knife edge, and then top clamped edge. Corresponding finite element predictions were also obtained that simulated the installation of the panel in the fixture.

Results that illustrate the predicted changes in geometry of the flat aluminum panel (AL-FLAT-2) subjected to the test-fixture boundary conditions are shown in figure 9. Figures 9(a), 9(b), 9(c), and 9(d), correspond to the sequential application of the boundary conditions in the following order: bottom clamped edge, right knife edge, left knife edge, and then top clamped edge, respectively. The measured geometry of the test specimen was found to be very different from the predicted geometry. The following measurements of the panel geometry were obtained from the panel at locations 1/8 in. above the bottom clamping plates and are marked with **X** symbols in figure 9(a)

Y coord. (in.) :	-5.8	-3.0	0.0	3.0	5.8
w measured (in.) :	0.00059	-0.00029	-0.00063	-0.00024	0.00057
w predicted (in.) :	0.00043	0.00044	0.00041	0.00035	0.00034

The data indicates that the panel is bowed just above the clamped end, which is assumed flat. The set of clamping plates for the flat panels was measured in the CMM and was determined to be flat within ±0.0001 in. Thus, it was first suspected that the panel was not being clamped firmly enough, but tightening the clamping plates did not change the panel geometry. The panel was then reversed in the fixture and the out-of-plane deformation was measured at the same locations just above the bottom clamped end. The following out-of-plane displacement values were obtained and indicate a similar bow in the panel, but appears reversed.

Y coord. (in.) :	-5.8	-3.0	0.0	3.0	5.8
w measured (in.) :	-0.00093	-0.00001	0.00131	0.00116	-0.00154
w predicted (in.) :	-0.00043	-0.00044	-0.00041	-0.00035	-0.00034

Thus, the clamping plates do not seem to have any bias in their geometry, they are just not fully removing the geometric imperfection along the clamped edge in this case. A second measurement of the actual in-

the-fixture panel geometry was verified by using the VIC-3D system and the results are shown in figure 10. The results indicate that the predicted initial in-the-fixture geometry (figure 9) is completely different from the measured geometry and also show the initial outward bow in the panel indicated by the previous measurements.

Upon further examination of the clamping plates, it is believed that a manufacturing anomaly in the clamping plates is causing the discrepancy between the predicted and measured in-the-fixture shape of the panel. More specifically, the clamping plates were originally machined with a radius on the top corner of the bearing surface to prevent the sharp corner from digging into the panel during testing. The set of clamping plates for the flat panels were accidentally machined with too large of a radius on this corner, and the rounded edge extended across a quarter of the clamping surface, as illustrated in figure 11. Even though the clamping plates were re-machined with the wire EDM process, this rounded edge condition still existed. Thus, the actual fixture boundary condition is acting over a smaller area of the panel and the assumed boundary conditions used in the finite-element model are not accounting for this discrepancy.

Since the STAGS finite-element analysis was incorrectly predicting the shape of the panel in the fixture, presumably due to the bad clamping plates, the predicted compression response of the panel was subsequently incorrect also. The predicted out-of-plane center displacement, δ, from the finite-element analysis is shown in figure 12 and compared with the experimentally measured value. The finite-element analysis indicates slight out-of-plane deformations in the pre-buckling range of loading and large magnitude outward deformations in the postbuckling range of loading. In contrast, the experimental results show the panel deforming inward with large magnitude pre-buckling displacements from the onset of loading. The inward deformation under load is not surprising, since the CMM measurements and VIC-3D measurements showed the panel to have an inward bulge after being clamped into the fixture prior to loading, as shown in figure 10.

An additional STAGS finite-element analysis was conducted to simulate the effects of the imperfect clamped boundary condition on the top and bottom loaded edges of the panel caused by the rounded edge of the clamping plates. As discussed above, the original finite-element analysis deformed the panels to match the idealized geometry of the fixture. However, if the initial geometric imperfection of the panel was only partially removed, as the measurements seem to suggest, then the panel might obtain an inward bulge-like shape similar to the observed in-the-fixture geometry. The measured out-of-fixture geometric imperfection of the panel consisted of an inward bulge with a magnitude of 0.040 in. The measured in-the-fixture panel geometry indicates a bulge of approximately 0.016 in. as shown in figure 10. Thus, it was assumed that the clamping plates removed approximately sixty percent of the imperfection. A finite-element analysis was performed in which sixty percent of the fixture-induced displacements were applied along the panel edges. The predicted initial geometry and compression response were very similar to the measured results. In particular, a plot of the out-of-plane center displacement of the panel using this modified boundary condition is shown in figure 12. The predicted in-the-fixture panel geometry now indicates a bulge with similar shape and comparable magnitude to the measured out-of-plane deformation shown in figure 10. The corresponding predicted out-of-plane deformation for the panel mounted in the fixture prior to loading is shown in figure 13. In summary, the results from the analysis with the modified boundary condition agree quite closely with the experimental values and illustrate how important it is to correctly characterize and model the experimental boundary conditions.

Next the corresponding curved aluminum panel (AL60-1) was examined. Results that illustrate the predicted changes in geometry of panel AL60-1 due to the application of test-fixture boundary conditions are shown in figure 14. Figures 14(a), 14(b), 14(c) and 14(d) correspond to the sequential application of the boundary conditions in the following order: bottom clamped edge, right knife edge, left knife edge, and then top clamped edge, respectively. The bottom clamped edge was secured first and measurements of the panel geometry were made at five points along the panel 0.125 in. above the bottom

clamping plate (marked by the **X** symbols in the figure). The measured and predicted results are summarized in the following table

Y coord. (in.) :	-5.8	-3.0	0.0	3.0	5.8
w measured (in.) :	-0.13876	0.06743	0.14249	0.06777	-0.13894
w predicted (in.) :	-0.13849	0.06745	0.14250	0.06745	-0.13849

These results show good agreement between the measured and predicted values, with less than 0.0005-in. difference. Similarly, geometry measurements were taken along horizontal lines at four locations when the panel was fully clamped. The horizontal measurements were vertically located at the mid-plane of the panel, ±3.0 in. from the mid-plane, and 5.88 in. above the mid-plane, as indicated by the dashed lines in figure 14(d). The out-of-plane deformation along these locations is shown in figure 15 and demonstrates the agreement between test and prediction for the initial geometry. The fact that the lines do not converge towards x = -7.0 in. indicates that the left knife edge was not aligned perfectly vertical. This correlates with results discussed earlier that indicated that the left knife edge was tilted 0.046° towards the panel front (or about 0.010 in. from top to bottom of the knife edge).

Overall, the analysis to simulate the effects of the fixture-induced changes in the panel geometry appears to work well when the fixture geometry is well characterized. Thus, it is reasonable to expect good correlation between the predicted and measured results for all of the curved panels that use the same type of clamping plates.

One other item that was noted during the setup and measurement of the panel in the fixture is that the knife-edge blades were discovered to be more flexible than previously known. While the knife edge blades are made of steel and seem very stiff, it is quite easy to cause them to bend a few thousandths of an inch by adjusting the knife-edge blade set screws unevenly. How much effect an uneven knife edge would have on the loaded response will likely depend on the particular panel, but it is something that should probably be avoided as much as possible, since it would be hard to quantify the curvature in the knife edge without measuring it. Because of this flexibility, the verticality of the knife edge should be measured at more than just two points. Measurement at five positions located from top to bottom should be sufficient to ensure that the knife-edge is relatively straight.

Effects of test-fixture-induced friction

Based on previous experience, a significant portion of the observed discrepancies between test and analysis results can be attributed to test-fixture-induced friction along the loaded edges. However, the effects of test-fixture-induced friction and other nontraditional boundary conditions have not been discussed to a great extent in the literature, presumably because in many cases they have little effect on the response of compression-loaded panels. In addition, most analytical models assume free expansion of the panel in the circumferential direction (N_{xy} = 0) because of solution difficulties associated with prescribing the v = 0 boundary condition. Specifically, setting the circumferential displacement equal to zero along the loaded edges (v = 0) while having free expansion of the side edges results in a singularity at the corners. This is not a limitation for finite-element analyses, but choosing between the two boundary conditions is somewhat arbitrary without knowledge of the as-tested boundary conditions. For curved panels, when the circumferential displacement is equal to zero along the loaded edges, the panel deforms outward when it is loaded in axial compression. Depending on the geometry and properties of the panel, this outward deformation can sometimes be large enough to retard or prevent the inward snap-through of the panel.

Several examples illustrating the different response characteristics exhibited by compression-loaded aluminum panels with $v = 0$ or $N_{xy} = 0$ boundary conditions are shown in figure 16. These predicted results are based on finite-element models that use the same nominal thickness, length, and arc-width as the panels discussed in the previous sections. For the flat panels, the two different boundary conditions create very similar load versus center displacement responses, as shown in figure 16(a). There is, however, a 5% difference in the buckling load for the flat panel. The corresponding response of a 15-in-radius curved panel is shown in figure 16(b). In this case, there is a difference in the magnitude of out-of-plane deformation, but the buckling loads are very similar. When large cutouts are present in the panel, the difference caused by the two boundary conditions is often negligible as shown for a 60-in-radius aluminum panel with a 7-in-diameter circular cutout in figure 16(c). However, the load versus center displacement for a 60-in-radius panel with no cutout varies significantly for the $v = 0$ and $N_{xy} = 0$ boundary conditions (figure 16(d)). In particular, the panel has a monotonically increasing stable response similar to a flat panel when the $v = 0$ condition is used. In contrast, the panel has much smaller magnitude out-of-plane displacements prior to collapsing inward when the $N_{xy} = 0$ condition is used. In references 7 and 8, cases are noted where a shallow curved panel does collapse inward with the $v = 0$ condition, but the collapse occurs at higher load levels than when the edges are free to expand. While it is not difficult to model the $v = 0$ condition along the loaded edges with finite-element methods, it was deemed preferable to achieve free expansion during the experimental tests so that the test results could be used to validate analytical predictions from models that assume the $N_{xy} = 0$ boundary condition.

A test method development activity was initiated to develop and verify methods to reduce test-fixture-induced friction effects observed in tests. Two curved aluminum panels, AL60-1 and AL60-2, were tested and measurements with DCDTs were made to verify that the panel was sliding laterally relative to the fixture. The outward lateral displacement near the top of the panel was measured using a set of DCDTs as shown in figure 1. Several layers of material were placed between the loaded edges of the panel and the fixture to help reduce the coefficient of friction along the loaded edges including 0.003-in-thick Teflon tape, 0.003-in-thick piece of aluminum shim stock and thin steel shim stock. A cross-sectional view of the resulting sandwich of materials is illustrated in figure 17. The Teflon layer was used to minimized the sliding friction, as suggested by Wilkens (ref. 10). The aluminum shim stock was used to help keep the composite fibers from penetrating the Teflon and embedding themselves in the steel. The steel shim stock was used to improve the smoothness of the loading plate surface and to facilitate sliding of the panel over the loading surface.

Experimentally measured and numerically predicted load-displacement results for the curved panel AL60-1 are shown in figure 18. The load versus out-of-plane center displacement response curves are shown in figure 18(a), load–end-shortening response curves are shown in figure 18(b), and load versus lateral expansion response curves are shown in figure 18(c). The lateral expansion is calculated from the measurements obtained by two DCDTs mounted to the sides of the panel. One DCDT on each side of the panel measured the circumferential expansion of the panel 0.25 in. from the top edge, and these measurements were added together to give the total lateral expansion. In each of these figures the experimental results (thick solid line) are depicted along with the STAGS finite-element results for $N_{xy} = 0$ (thin solid line) and $v = 0$ (dashed line). The corresponding results for panel AL60-2 are shown in figure 19.

For both the AL60-1 and AL60-2 panels the STAGS analyses with $N_{xy} = 0$ predicted panel collapse, while the analyses with $v = 0$ predicted that the panel would have a monotonically increasing stable response with large outward deformation. The experimental results shown in figure 18 for the AL60-1 panel indicate that the panel is neither fully restrained nor fully free to slide at the loaded edges. The magnitude of the out-of-plane center displacement is not as large as the displacement predicted by the STAGS model with $v = 0$, but the panel did not collapse inward like the model with $N_{xy} = 0$. The end shortening response for the experiment and the two STAGS models are all very similar. The offset in the experimental data is a result of gear lash in the load frame and the imperfection of the panel's loaded

edges. The imperfection along the loaded edges results in the panel initially contacting the loading plate at only a few points, and then as the load increases the contact area increases, thus resulting in a nonlinear load-end-shortening response in the initial part of the response curves. The total lateral expansion measured during the experiment shows two distinct behaviors. At relatively low load levels, the panel appears to expand freely, but as load increases the expansion rapidly decreases to match the expansion rate of the STAGS model with $\nu = 0$. The reason that the $\nu = 0$ model predicts a small amount of expansion as opposed to zero expansion is because the measurement of the lateral displacement is taken at 0.25 in. from the top of the panel rather than precisely at the top edge, and this location exhibits some lateral expansion. The results shown in figure 19 for the AL60-2 panel indicate similar behavior, with the only exception being that the panel still collapsed inward in spite of the large outward center displacement. The determining factor for whether each panel collapsed was most likely the difference in the imperfection shapes between the two panels.

Based on the results for these two panels, it seems that the boundary condition created with the combination of Teflon, steel and aluminum is not the ideal $N_{xy} = 0$ condition that was desired. Since the results indicated that some sliding was occurring along the loaded edges, the AL60-1 panel was tested three more times with small modifications to the experimental setup in order to further reduce test-fixture-induced friction. However, it was determined that none of the attempts to create a free expansion condition along the loaded edges were fully successful. Thus, it was decided that, while the $\nu = 0$ boundary condition was not ideal, it would at least allow repeatable correlation between the STAGS finite-element-modeling methods and the experimental results. To demonstrate this, panel AL60-1 was tested again with no Teflon or shim stock between the edges of the panel and the fixture loading plates. The results for this test are shown in figure 20 along with the STAGS finite-element results for $N_{xy} = 0$ and $\nu = 0$. The measured out-of-plane center deflection agree well with the STAGS results that assume the $\nu = 0$ boundary condition. Similarly, the measured and predicted end shortening and lateral displacement response agree well as shown in figs. 20(b) and 20(c), respectively. Although this set of tests with the aluminum panels failed to produce a test setup that would allow the panel to freely expand under load, it did demonstrate that the response of shallow curved panels can be modeled accurately by using the $\nu = 0$ boundary condition in a STAGS finite-element model.

Effects of nonuniform load introduction

Several studies in the literature indicate that the response of compression-loaded thin-walled shells can be sensitive to nonuniform load introduction affects and motivated the study of this sensitivity in this work.[1] Nonunifom load introduction in a panel specimen is attributed to initial specimen-end or loading-surface imperfections, and test-fixture-induced inplane geometry changes. The edge imperfection is typically created when the panel is fabricated. The test-fixture-induced inplane deformation is caused by clamping a geometrically imperfect panel into the test fixture. Specifically, when the panel is clamped in the fixture any out-of-plane imperfection is removed in the clamped sections and along the knife edges. This clamping can induce an inplane displacement prior to the panel being loaded. The effects of these types of end imperfections were studied and the results are presented in this section.

The unrestrained or out-of-fixture end imperfection was measured by using a CMM. This measurement was used to quantify the end imperfection variation across the width of the panel and through the thickness. The aluminum panels were shown to be relatively flat through the thickness (±0.0002 in.) and had only a small variation across the width of the panel (approx. ±0.001 in.). The test-fixture-induced end imperfection was predicted in STAGS by using a similar procedure used to predict the test-fixture-induced panel geometry changes described in an earlier section. In this case, a flat aluminum panel with geometry similar to AL-FLAT-2 was modeled and was assumed that geometric imperfection was the same shape as AL-FLAT-2, but had a magnitude of approximately 0.040 in. to simulate a "worst case" imperfection that would induce a "worst-case" test-fixture-induced end imperfection. The predicted induced end imperfection was less than 0.0001 in. across the width of the

panel and since this variation is an order of magnitude smaller than any measured edge imperfection due to machining, it was neglected during analysis.

Results from a subsequent finite-element analysis of this configuration that included the effects of the measured end imperfection indicated that this particular imperfection had no noticeable affect on the panel response. In addition, the other aluminum and composite panels were measured and the end imperfections appeared to be no greater than ±0.001 in. in magnitude. Thus, the end imperfection was neglected in future analysis of these particular panels.

Recommendations

Some of the possible errors affecting high-fidelity modeling and testing of compression-loaded panels and how these errors can be quantified and minimized were presented. Overall, the testing and measurements verified that high-fidelity modeling of the experimental setup is possible, and that the modeling methods accurately predict the load-displacement response observed in the tests. However, the authors were not able to achieve the goal of creating an experimental setup that allowed the testing of compression loaded panels with free expansion along the loaded edges as desired. The initial geometry of the panel when installed in the test fixture is very sensitive to fixture alignment and the geometry of the clamping plates used to enforce the clamped boundary condition on the loaded edges. Careful machining and measurement is required to ensure that the panel is held in the fixture as expected, and standard machining tolerances may not be sufficient to replicate the ideal boundary conditions. Finite-element analysis accurately predicts the test-fixture-induced specimen geometry when the panel geometry and imposed boundary conditions are measured and used along with the geometric imperfection. This enables the model to predict the initial geometry and pre-stress when the panel is installed in the fixture. The use of Teflon and steel shims between the loaded edge of the panel and the load bearing surfaces failed to reduce the friction at the interface and create free expansion of the panel along the loaded edges in the circumferential direction. Test-fixture-induced friction between the fixture and the loaded edges of the specimen prevents circumferential expansion of the panel along the loaded edges during compression testing, but finite-element analyses can model this condition and produce accurate predictions of the panel response. Small-magnitude initial end imperfections (within ±0.003-in. manufacturing tolerance) have no noticeable affect on the response of the panels presented herein.

References

1. Hilburger, M. W.; and Starnes, J. H. Jr.: Effects of Imperfections on the Buckling Response of Composite Shells. *Thin-Walled Structures*, vol. 42, 2004, pp. 369-397.

2. Hui, D.: Asymmetric Postbuckling of Symmetrically Laminated Cross-ply Short Cylindrical Panels Under Compression. *Composite Structures*, vol. 3, 1985, pp. 81-95.

3. Snell, M. B.; and Morley, N. T.: The Compression Buckling Behaviour of Highly Curved Panels of Carbon Fibre Reinforced Plastic. *Proceedings of the Fifth International Conference on Composite Materials*, ICCM Volume 5, 1985, pp. 1327-1354.

4. Leissa, A. W.: *Buckling of Laminated Composite Plates and Shell Panels*. Report AFWAL-TR-85-3069, Air Force Wright Aeronautical Laboratories, June 1985.

5. Knight, N. F.; and Starnes, J. H. Jr.: Postbuckling Behavior of Selected Graphite-Epoxy Cylindrical Panel Loaded In Compression. *Proceedings of the AIAA/ASME/ASCE/AHS 27th Structures, Structural Dynamics, and Materials Conference*, San Antonio, TX, May 1986, AIAA paper 86-0881-CP.

6. Khot, N. S.; and Bauld, N. R., Jr.: A Numerical and Experimental Investigation of the Buckling Behavior of Composite Panels. *Computers and Structures*, vol. 15, no. 4, 1982, pp. 393-403.

7. Hilburger, M. W.; Britt, V. O.; and Nemeth, M. P.: Buckling Behavior of Compression-Loaded Quasi-Isotropic Curved Panels With a Circular Cutout. *International Journal of Solids and Structures*, vol. 38, 2001, pp.1495-1522.

8. Hilburger, M. W.; Nemeth, M. P.; Riddick, J. C.; and Thornburgh, R. P.: Compression-Loaded Composite Panels With Elastic Edge Restraints and Initial Prestress. NASA/TP-2005-213906, 2005.

9. Rankin, C. C.; Brogan, F. A.; Loden, W. A.; and Cabiness, H. D.: *STAGS Users Manual, Version 4.0*. Lockheed Martin Missiles & Space Co., Inc., Advanced Technology Center, Report LMSC P032594, May 2001.

10. Wilkins, D. J.: Compression Buckling Tests of Laminated Graphite-Epoxy Curved Panels. *AIAA Journal*, vol. 13, no. 4, 1975, pp. 465-470.

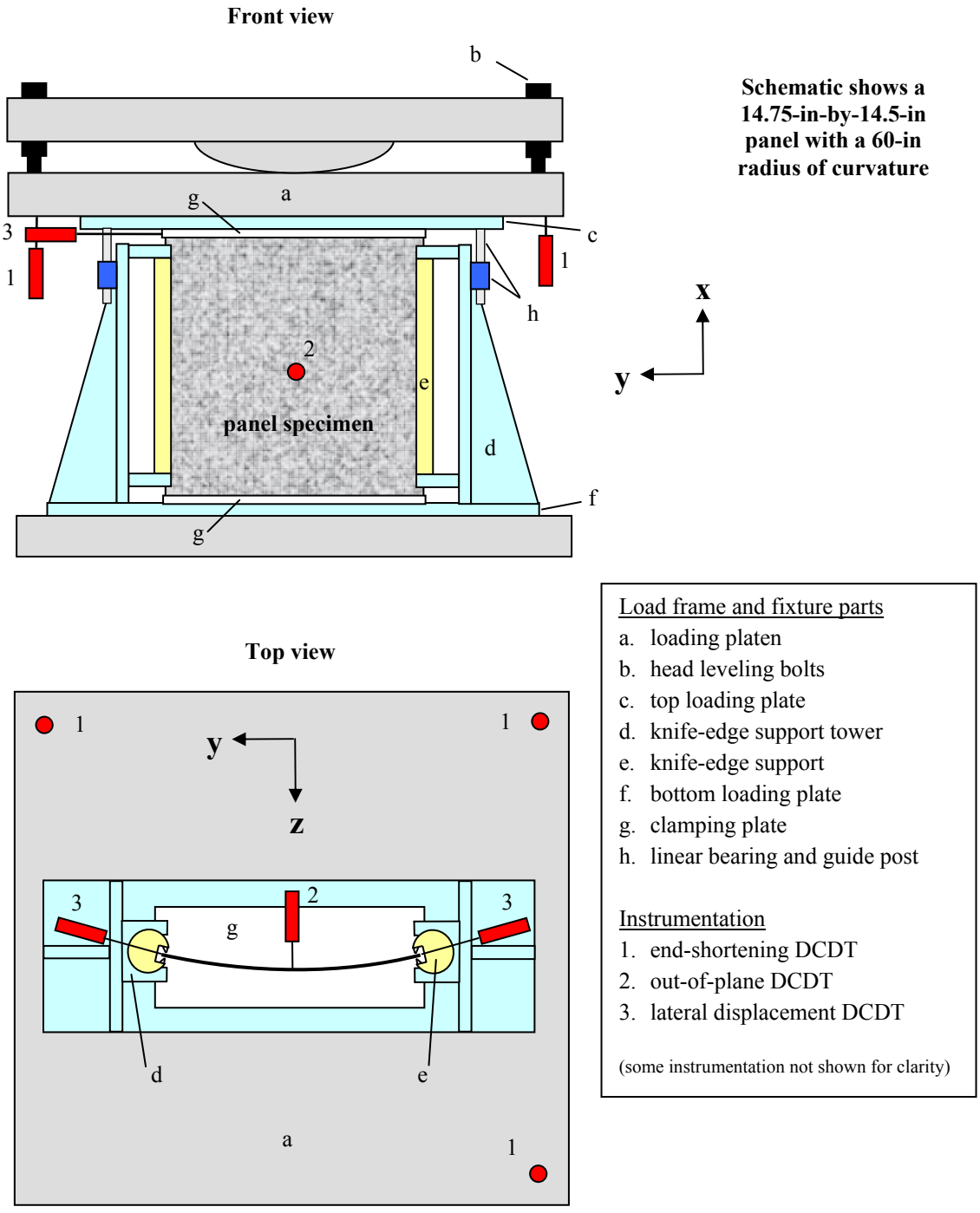

Figure 1. Test fixture and instrumentation setup for compression-loaded panels.

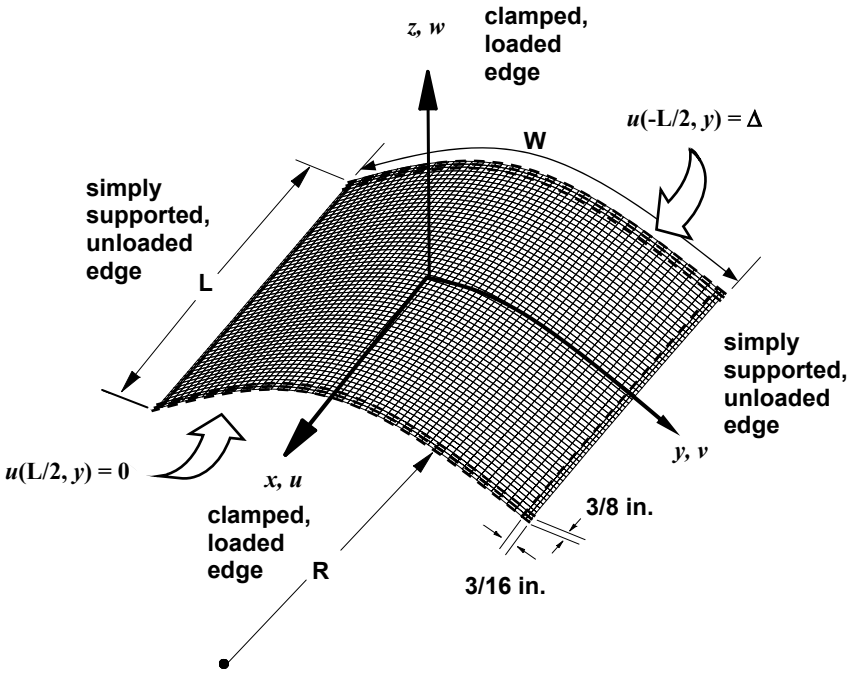

Figure 2. Typical model geometry and boundary conditions (dashed lines mark the rows and columns where the boundary conditions are applied).

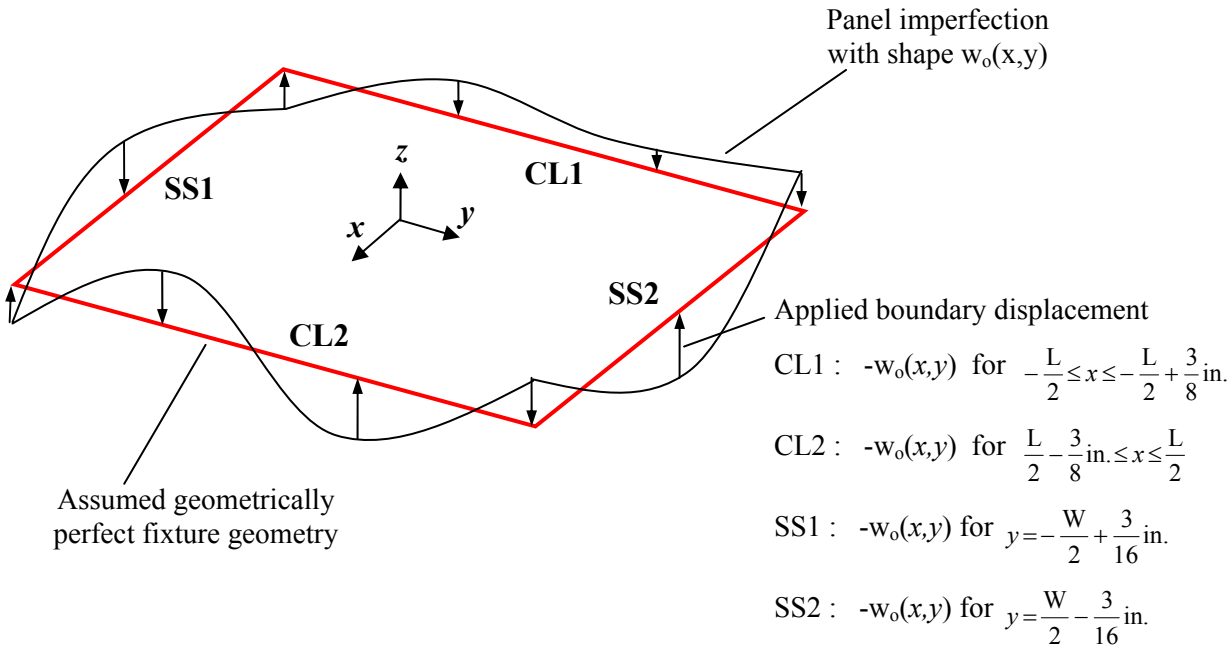

Figure 3. Finite-element boundary conditions based on measured panel imperfection.

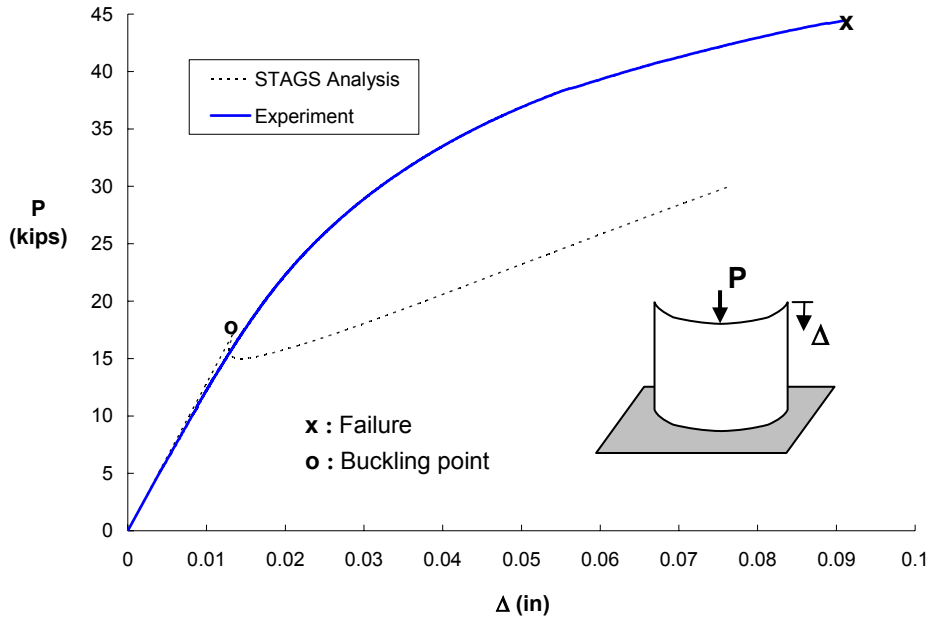

Figure 4. Comparison of STAGS finite-element analysis and experimental data for a compression-loaded $[0_2/+45/-45]_{3s}$ graphite-epoxy laminate with a radius-of-curvature of 60 in.

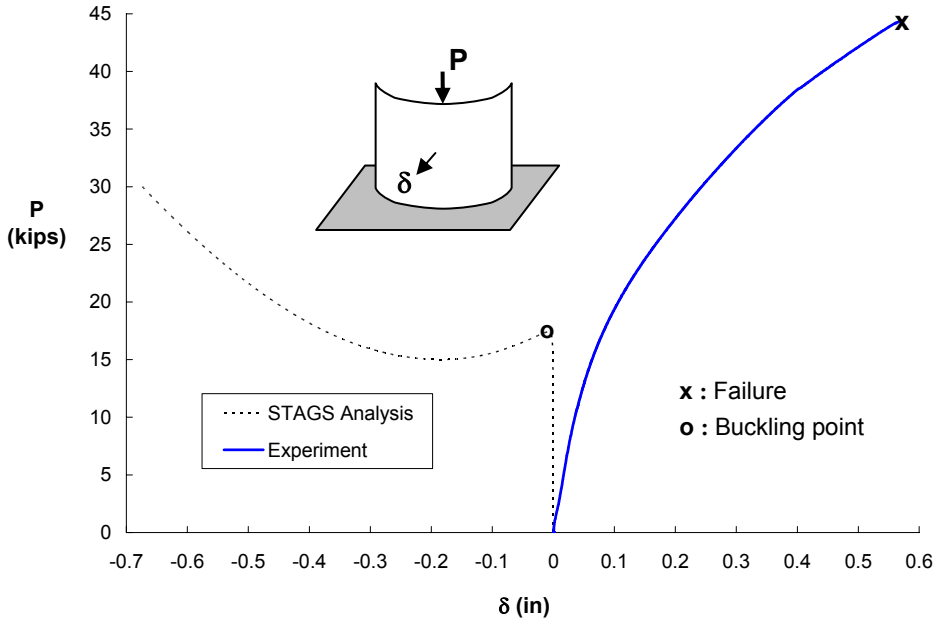

Figure 5. Comparison of STAGS finite-element analysis and experimental data for a compression-loaded $[0_2/+45/-45]_{3s}$ graphite-epoxy laminate with a radius-of-curvature of 60 in.

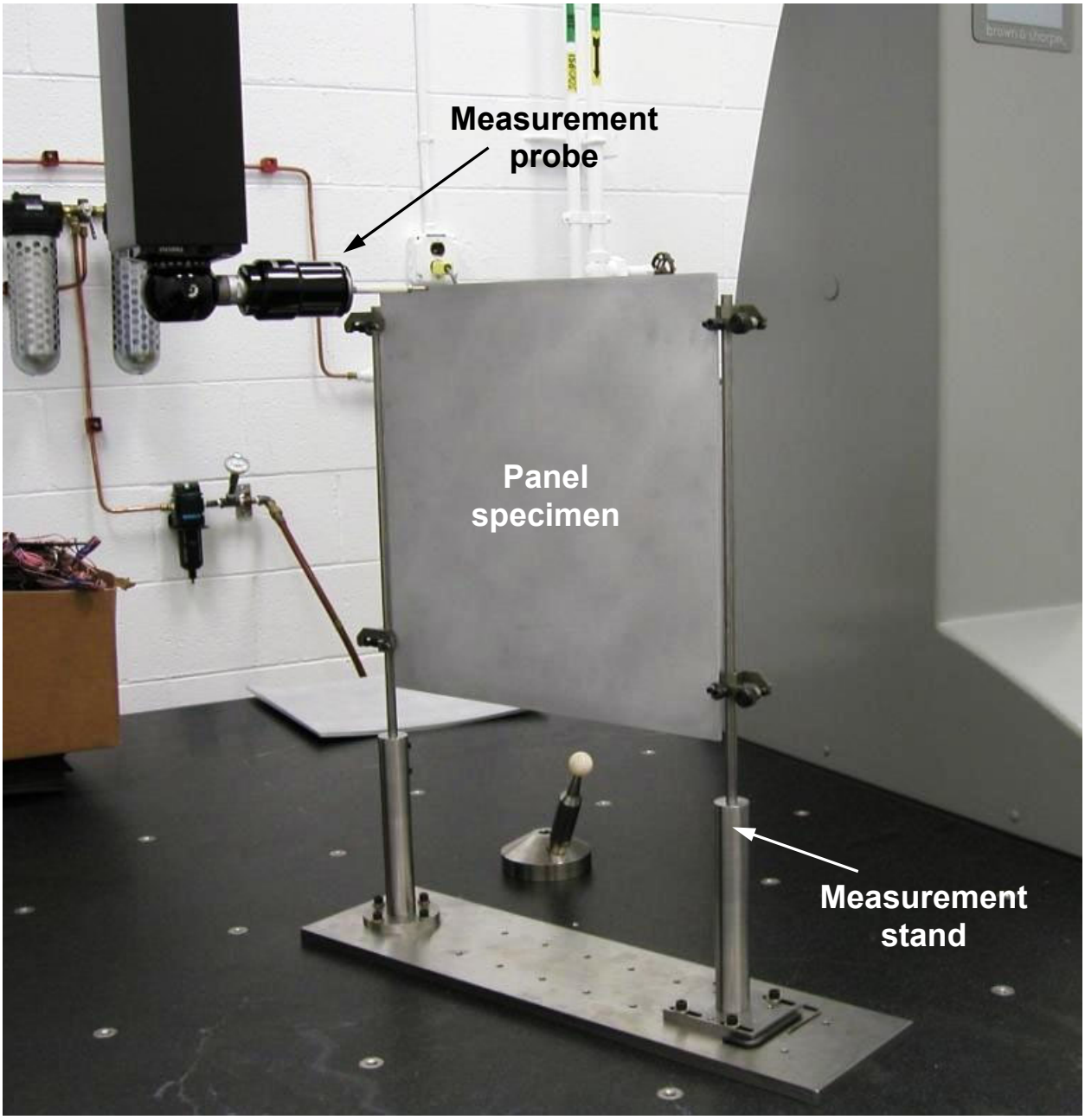

Figure 6. Measurement stand used for CMM measurements of flat and curved panels.

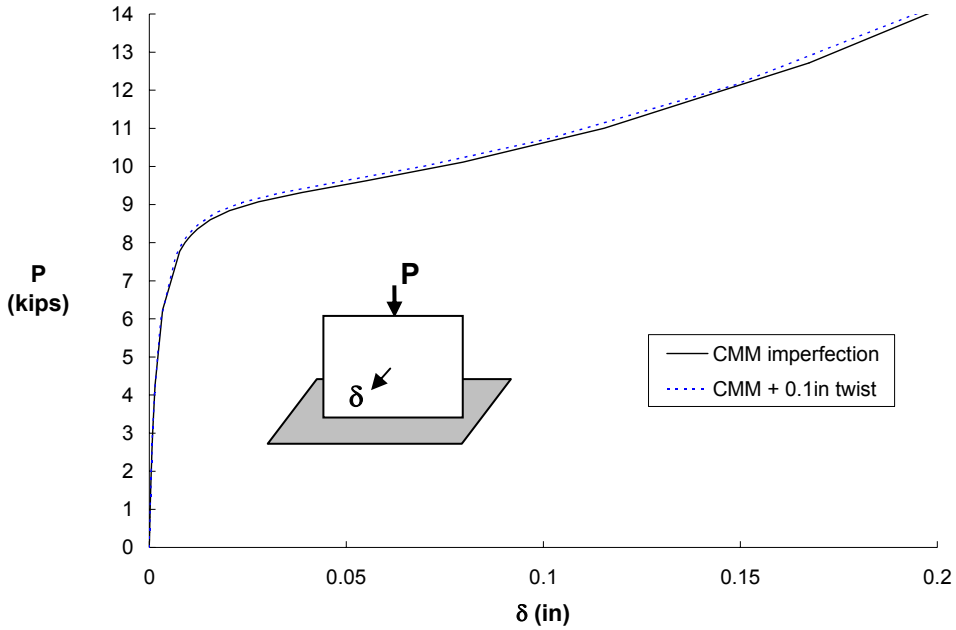

(a)

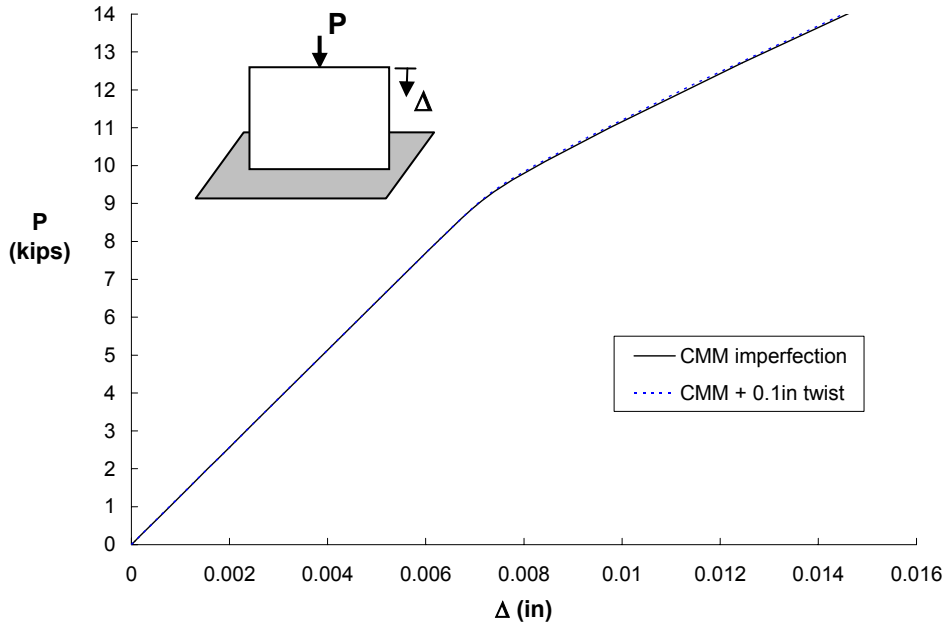

(b)

Figure 7. Out-of-plane center displacement (a) and end shortening (b) for a flat aluminum panel.

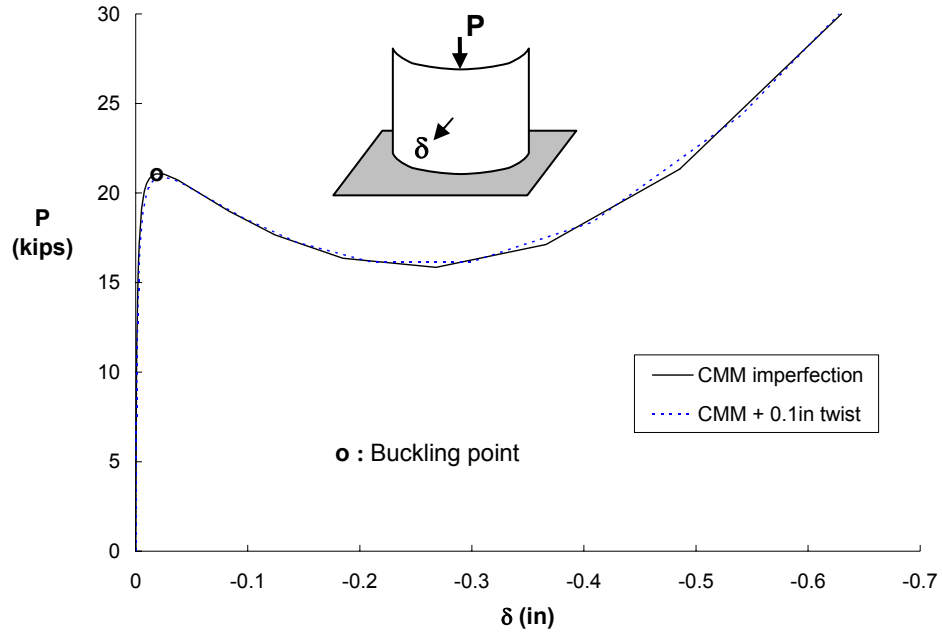

(a)

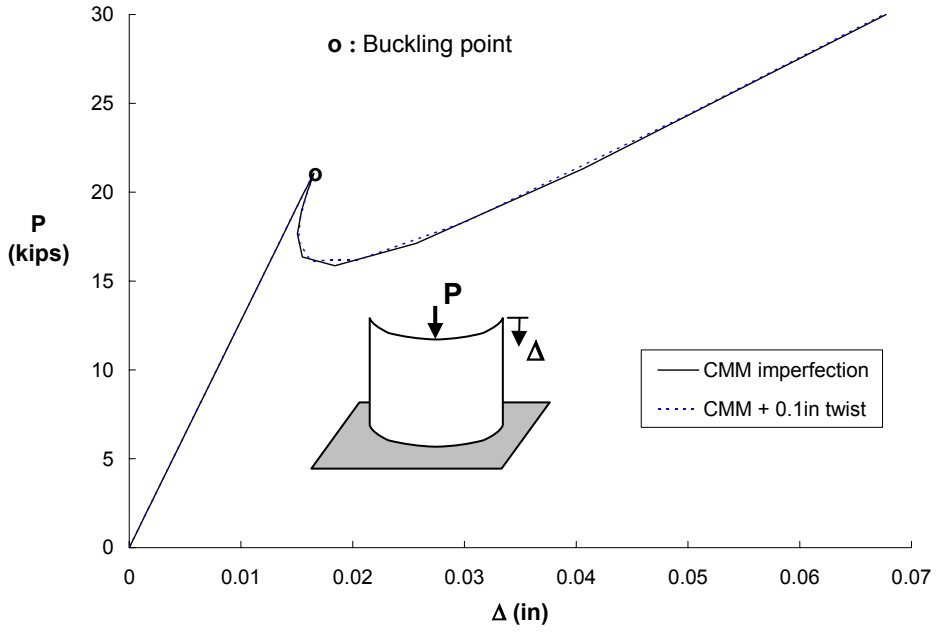

(b)

Figure 8. Out-of-plane center displacement (a) and end shortening (b) for a curved aluminum panel with a radius-of-curvature of 60 in.

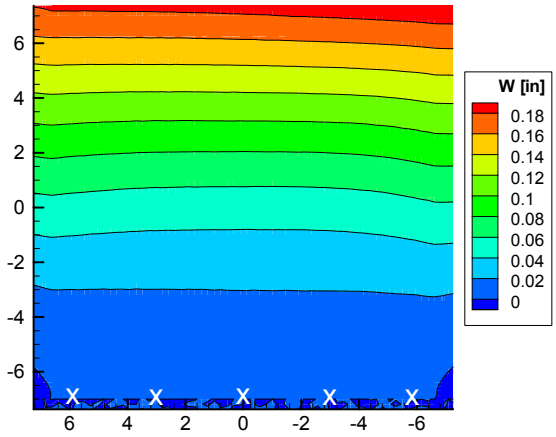

(a) Bottom edge clamped

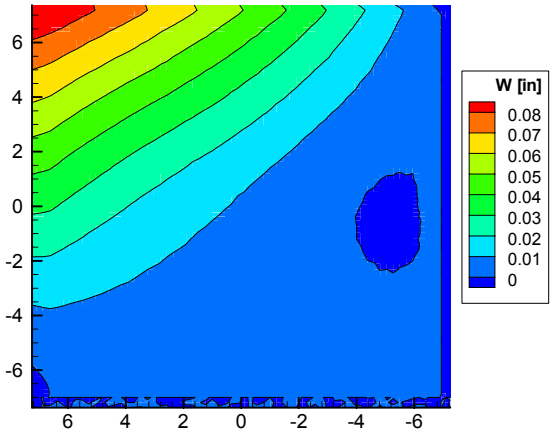

(b) Bottom and right edges clamped

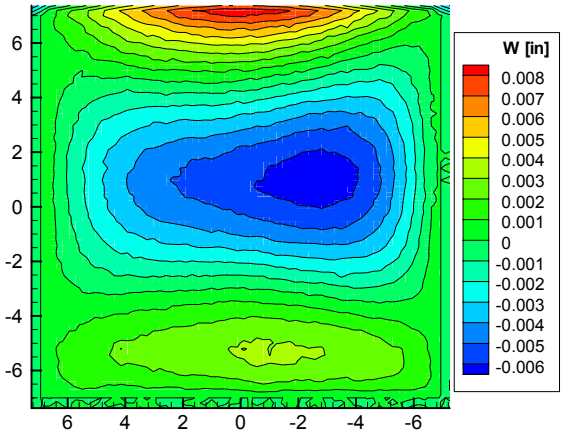

(c) Bottom and both sides clamped

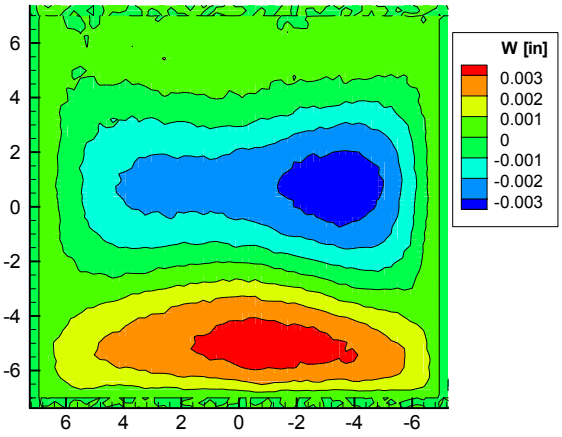

(d) All edges clamped

Figure 9. Finite-element predicted out-of-plane deformation of the flat aluminum panel during installation into fixture.

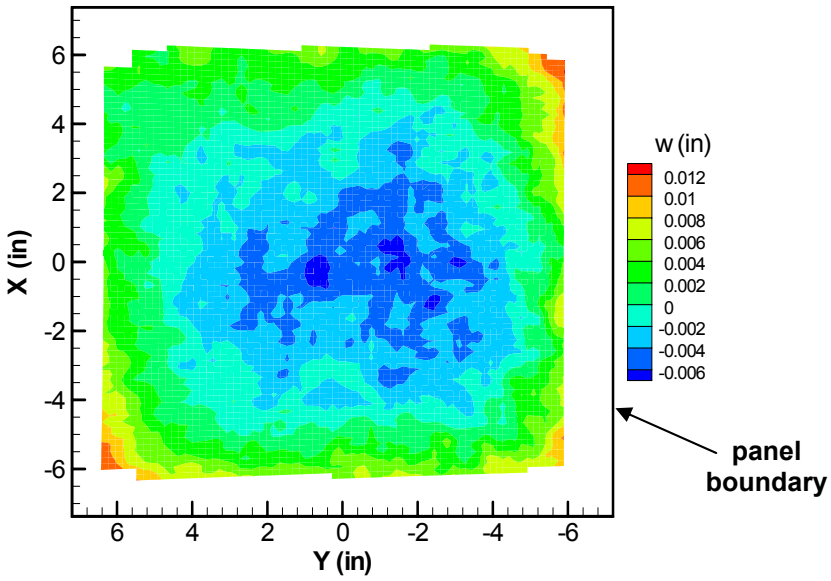

Figure 10. Out-of-plane deformation of flat aluminum panel AL-FLAT-2 prior to loading, as measured with the VIC-3D system.

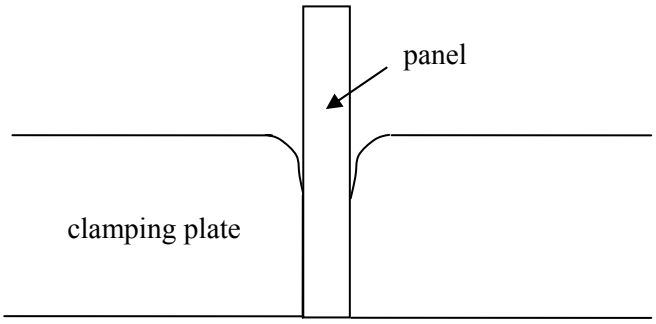

Figure 11. Schematic illustrating location of the rounded edges of the flat clamping plates.

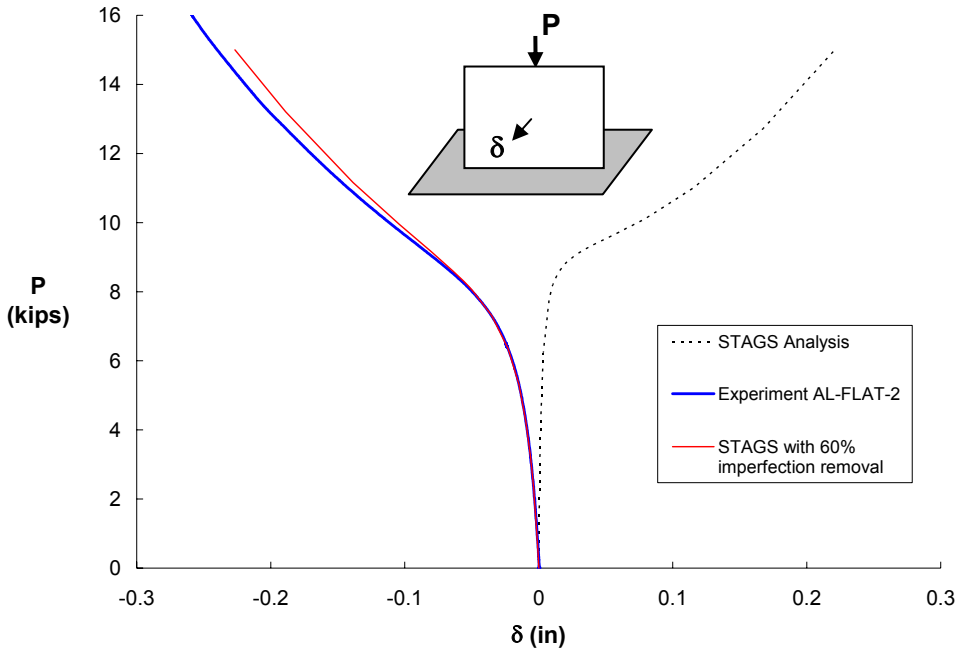

Figure 12. Comparison of the predicted and experimental out-of-plane center displacement for flat aluminum panel AL-FLAT-2.

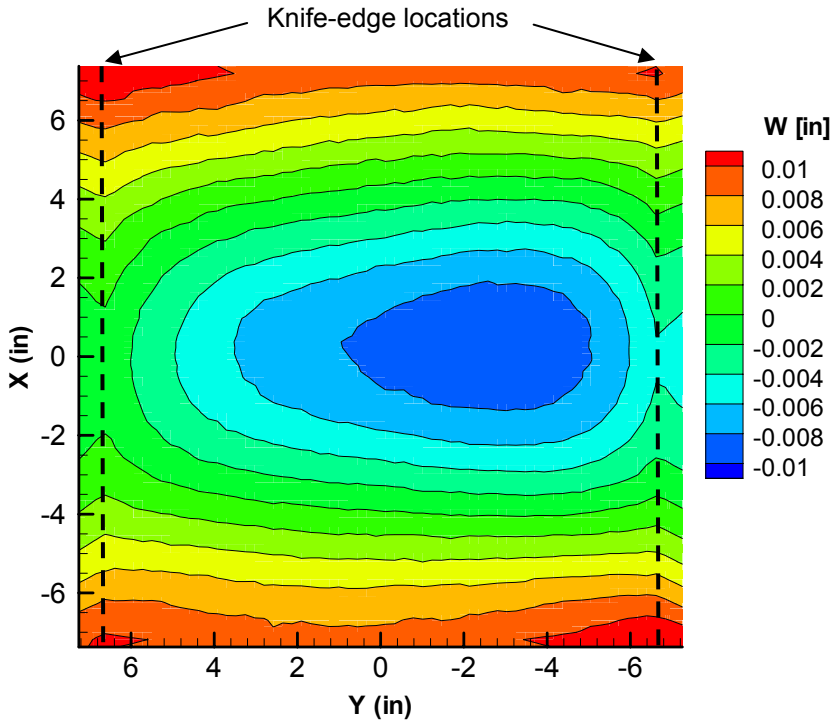

Figure 13. Out-of-plane deformation of flat aluminum panel AL-FLAT-2 prior to loading, assuming only sixty percent imperfection removal by the clamped edges.

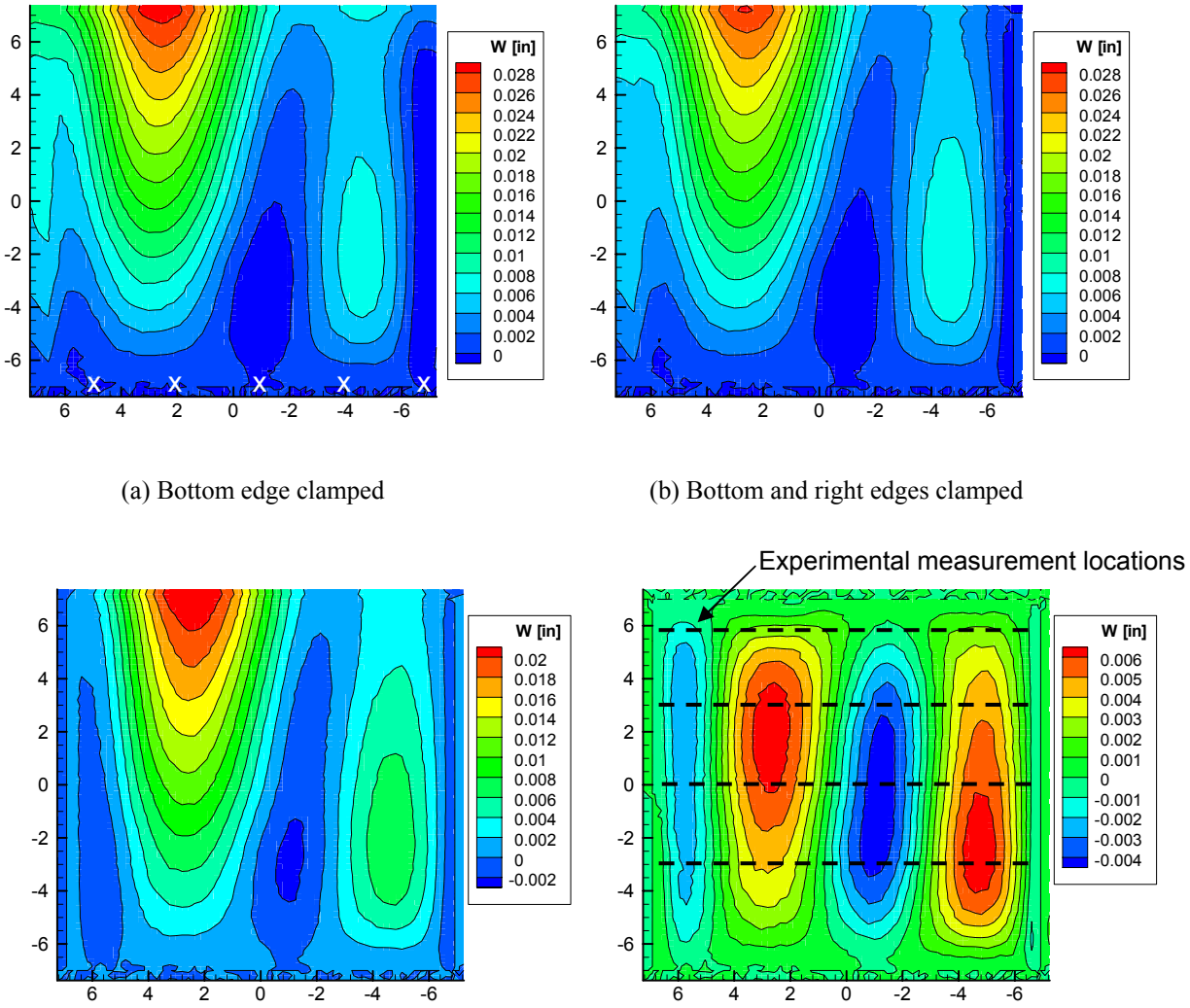

(a) Bottom edge clamped

(b) Bottom and right edges clamped

(c) Bottom and both sides clamped

(d) All edges clamped

Figure 14. Finite-element predicted out-of-plane deformation of the curved aluminum panel during installation into fixture.

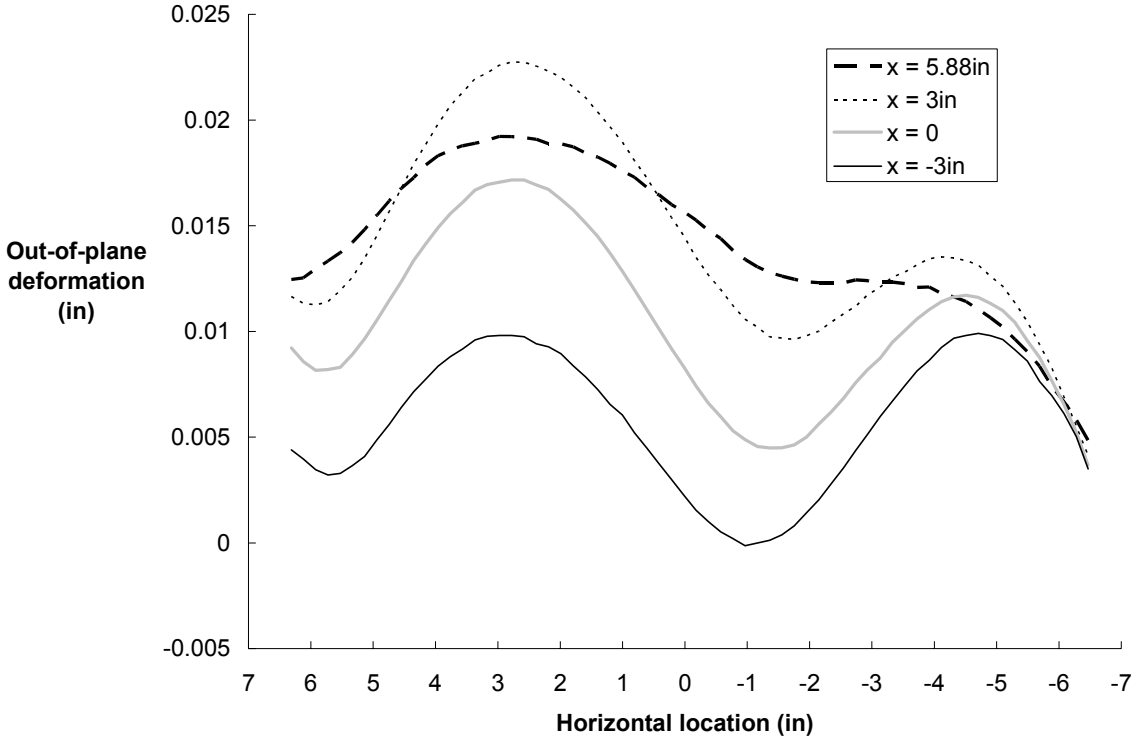

Figure 15. Measured out-of-plane deformation for curved aluminum panel AL60-1 in-fixture, prior to loading (see figure 14(d) for coordinate location).

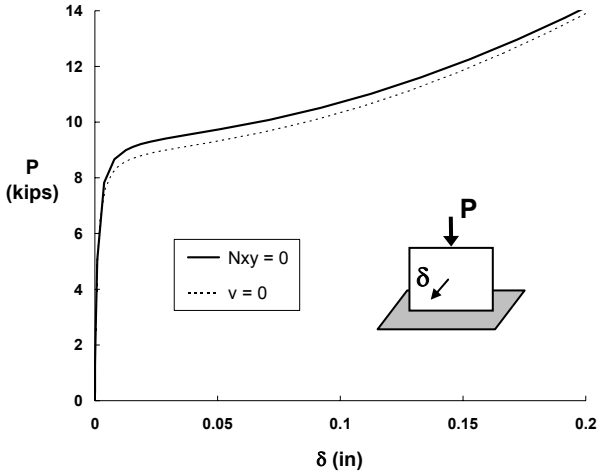

(a) Flat panel

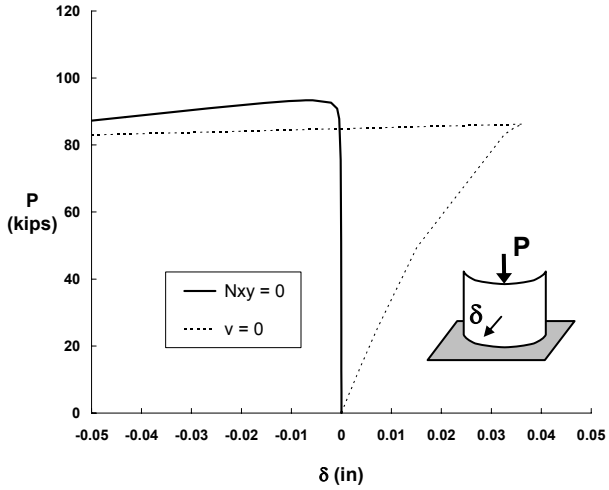

(b) 15-in-radius-of-curvature

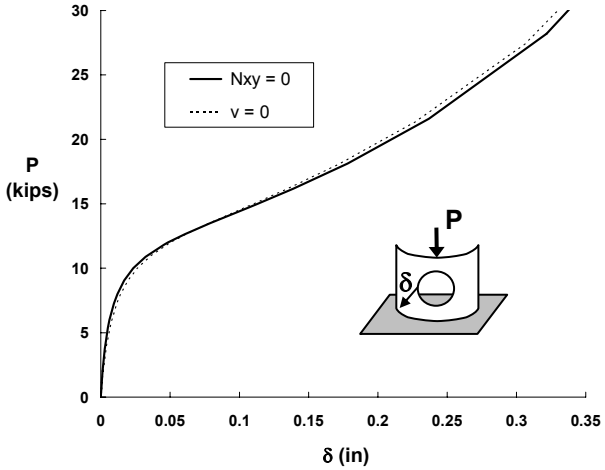

(c) 60-in-radius-of-curvature with cutout

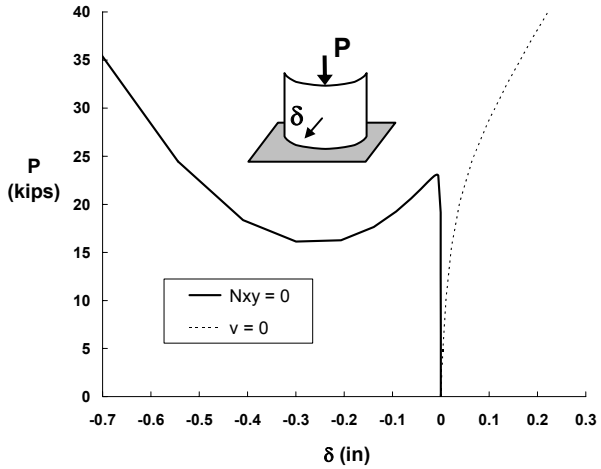

(d) 60-in-radius-of-curvature

Figure 16. Comparison between STAGS finite-element analysis results for aluminum panels with free expansion and zero expansion along loaded edges.

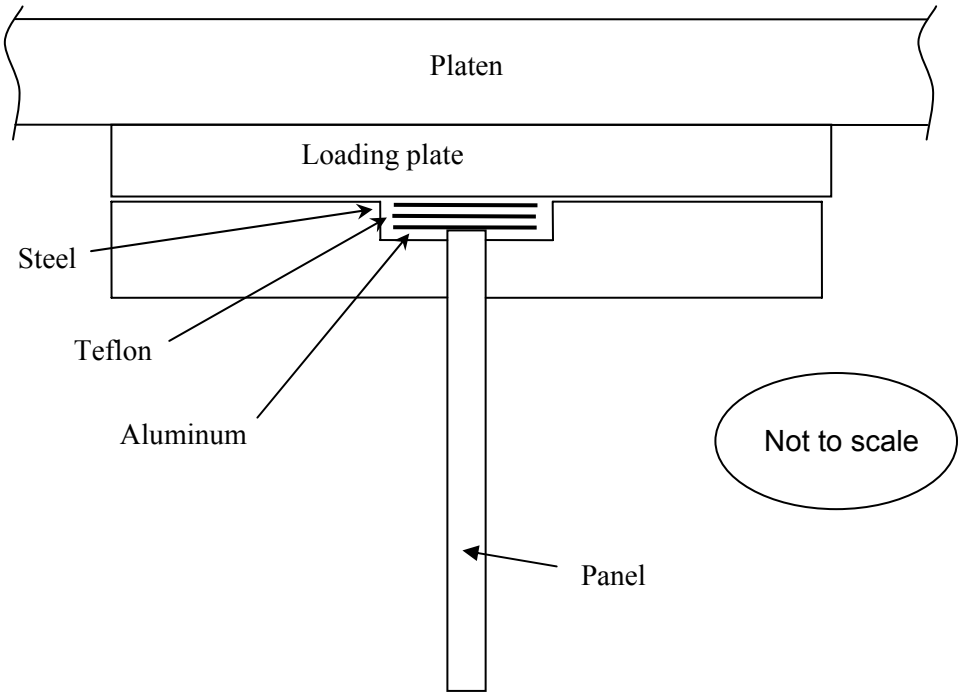

Figure 17. Schematic illustrating the cross-sectional view of materials used to facilitate free expansion of the panel along the loaded edges.

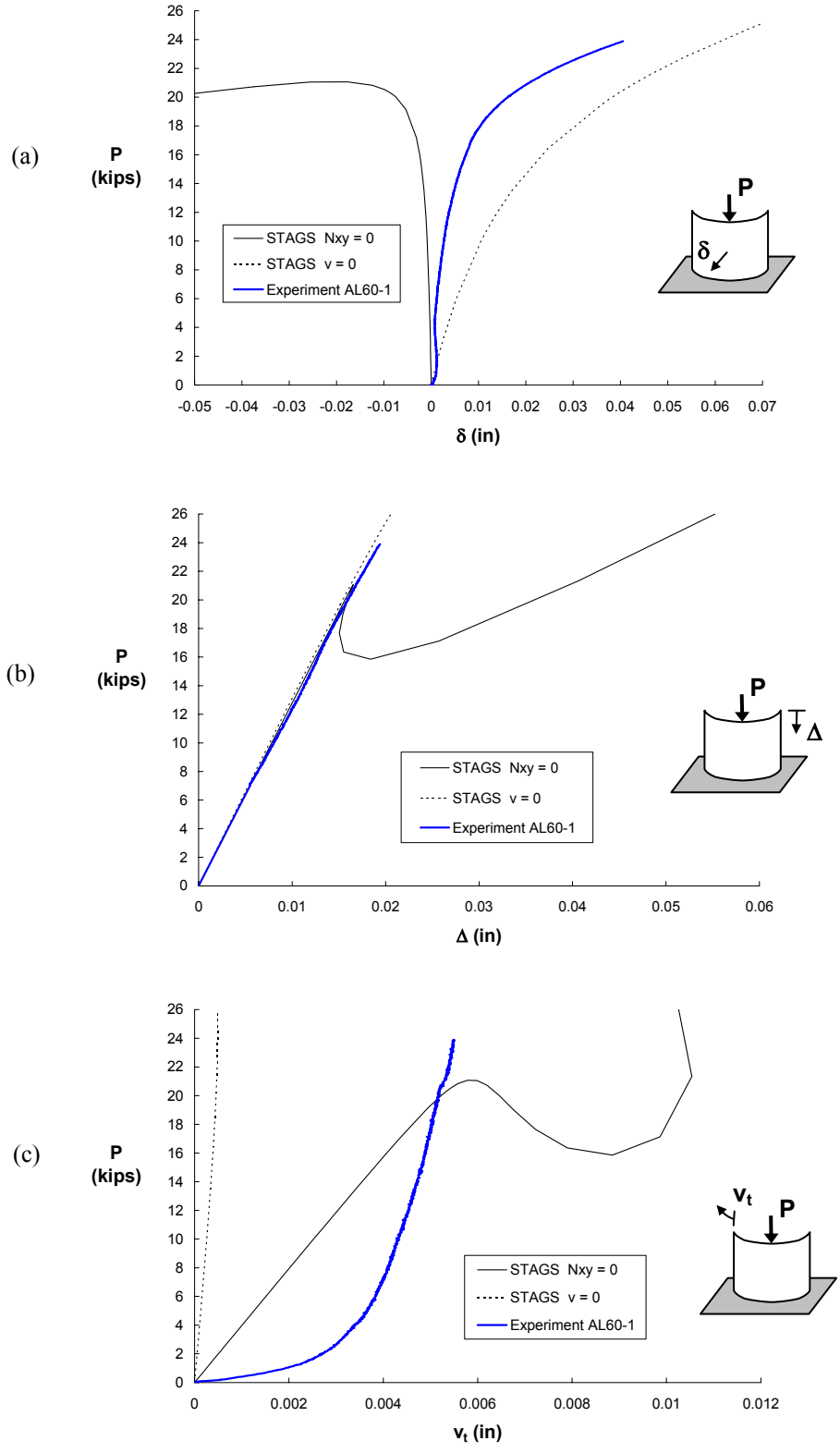

Figure 18. Comparison of experimental and STAGS finite-element results for the out-of-plane center displacement (a), end shortening (b), and total lateral displacement (c) of panel AL60-1.

(a)

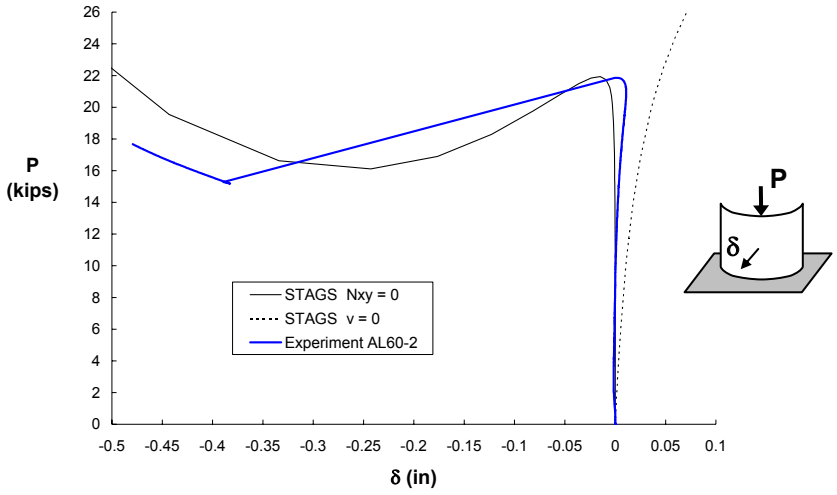

(b)

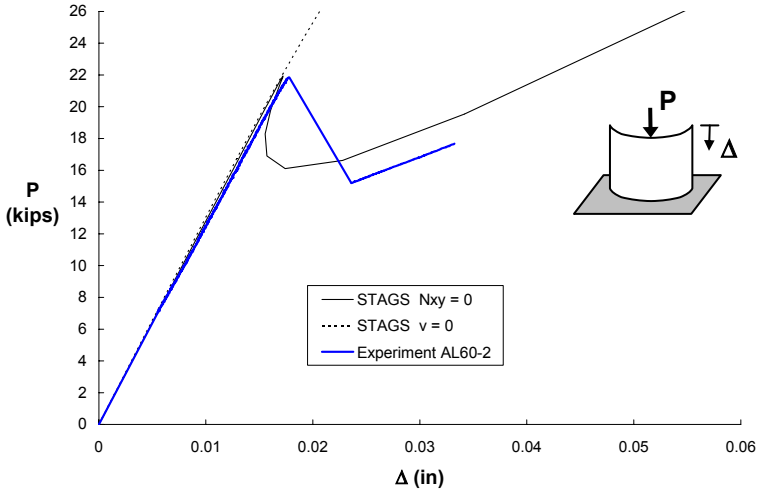

(c)

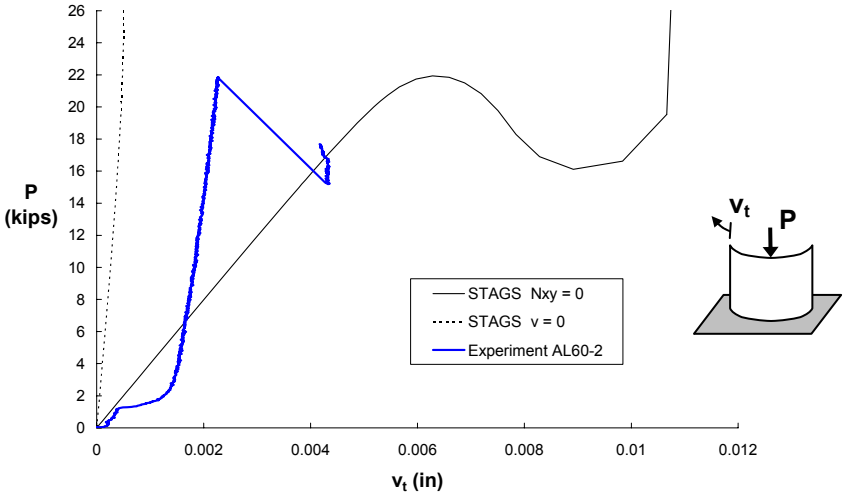

Figure 19. Comparison of experimental and STAGS finite-element results for the out-of-plane center displacement (a), end shortening (b), and total lateral displacement (c) of panel AL60-2.

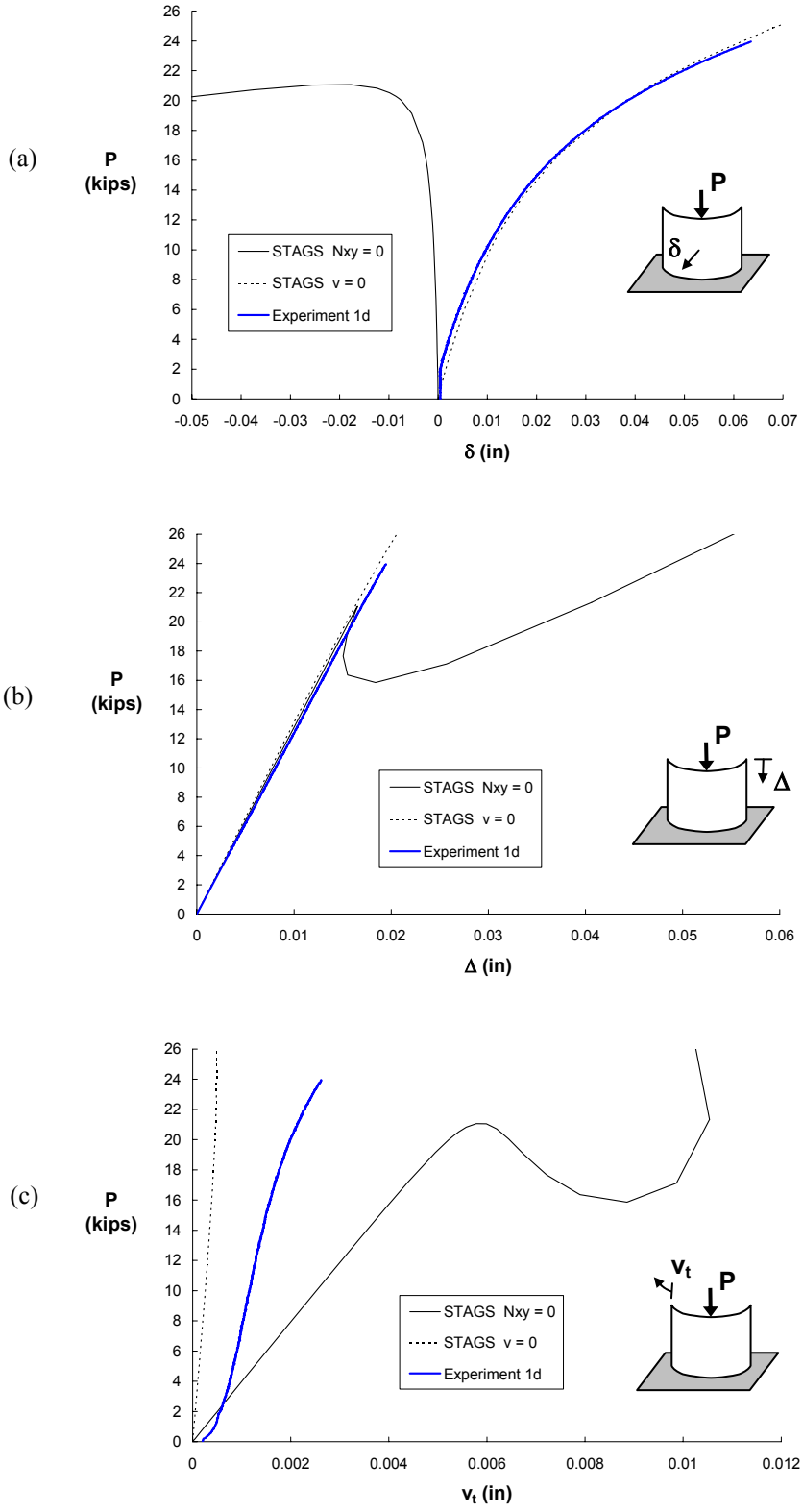

Figure 20. Comparison of the STAGS finite-element response with the experimental results for panel AL60-1 with unmodified edge conditions.

REPORT DOCUMENTATION PAGE

Form Approved
OMB No. 0704-0188

The public reporting burden for this collection of information is estimated to average 1 hour per response, including the time for reviewing instructions, searching existing data sources, gathering and maintaining the data needed, and completing and reviewing the collection of information. Send comments regarding this burden estimate or any other aspect of this collection of information, including suggestions for reducing this burden, to Department of Defense, Washington Headquarters Services, Directorate for Information Operations and Reports (0704-0188), 1215 Jefferson Davis Highway, Suite 1204, Arlington, VA 22202-4302. Respondents should be aware that notwithstanding any other provision of law, no person shall be subject to any penalty for failing to comply with a collection of information if it does not display a currently valid OMB control number.
PLEASE DO NOT RETURN YOUR FORM TO THE ABOVE ADDRESS.

1. REPORT DATE *(DD-MM-YYYY)*	2. REPORT TYPE	3. DATES COVERED *(From - To)*
01- 10 - 2005	Technical Memorandum	

4. TITLE AND SUBTITLE

Identifying and Characterizing Discrepancies Between Test and Analysis Results of Compression-Loaded Panels

5a. CONTRACT NUMBER

5b. GRANT NUMBER

5c. PROGRAM ELEMENT NUMBER

6. AUTHOR(S)

Thornburgh, Robert P.; and Hilburger, Mark W.

5d. PROJECT NUMBER

5e. TASK NUMBER

5f. WORK UNIT NUMBER

23-064-30-30

7. PERFORMING ORGANIZATION NAME(S) AND ADDRESS(ES)

NASA Langley Research Center
Hampton, VA 23681-2199

8. PERFORMING ORGANIZATION REPORT NUMBER

L-19184

9. SPONSORING/MONITORING AGENCY NAME(S) AND ADDRESS(ES)

National Aeronautics and Space Administration
Washington, DC 20546-0001

10. SPONSOR/MONITOR'S ACRONYM(S)

NASA

11. SPONSOR/MONITOR'S REPORT NUMBER(S)

NASA/TM-2005-213932 ARL-TR-3664

12. DISTRIBUTION/AVAILABILITY STATEMENT

Unclassified - Unlimited
Subject Category 39
Availability: NASA CASI (301) 621-0390

13. SUPPLEMENTARY NOTES

An electronic version can be found at http://ntrs.nasa.gov

14. ABSTRACT

Results from a study to identify and characterize discrepancies between validation tests and high-fidelity analyses of compression-loaded panels are presented. First, potential sources of the discrepancies in both the experimental method and corresponding high-fidelity analysis models were identified. Then, a series of laboratory tests and numerical simulations were conducted to quantify the discrepancies and develop test and analysis methods to account for the discrepancies. The results indicate that the discrepancies between the validation tests and high-fidelity analyses can be attributed to imperfections in the test fixture and specimen geometry; test-fixture-induced changes in specimen geometry; and test-fixture-induced friction on the loaded edges of the test specimen. The results also show that accurate predictions of the panel response can be obtained when these specimen imperfections and edge conditions are accounted for in the analysis. The errors in the tests and analyses, and the methods used to characterize these errors are presented.

15. SUBJECT TERMS

Buckling; Curved; Experiment; Friction; Panel

16. SECURITY CLASSIFICATION OF:			17. LIMITATION OF ABSTRACT	18. NUMBER OF PAGES	19a. NAME OF RESPONSIBLE PERSON
a. REPORT	b. ABSTRACT	c. THIS PAGE			STI Help Desk (email: help@sti.nasa.gov)
					19b. TELEPHONE NUMBER *(Include area code)*
U	U	U	UU	34	(301) 621-0390